Carbohydrate Polymers 88 (2012) 772–779

Contents lists available at SciVerse ScienceDirect

Carbohydrate Polymers

journal homepage: www.elsevier.com/locate/carbpol

Extraction of cellulose nanocrystals from mengkuang leaves (*Pandanus tectorius*)

Rasha M. Sheltami[a,b], Ibrahim Abdullah[a], Ishak Ahmad[a,*], Alain Dufresne[c], Hanieh Kargarzadeh[a]

[a] *Polymer Research Centre (PORCE), School of Chemical Sciences and Food Technology, Faculty of Science and Technology, Universiti Kebangsaan Malaysia, 43600 Bangi Selangor, Malaysia*
[b] *Chemistry Department, Faculty of Science, University of Garyounis, Benghazi, Libya*
[c] *Grenoble Institute of Technology, the International School of Paper, Print Media and Biomaterials (PAGORA), BP65, 38402 Saint Martin d'Hères Cedex, France*

ARTICLE INFO

Article history:
Received 2 December 2011
Received in revised form 17 January 2012
Accepted 19 January 2012
Available online 28 January 2012

Keywords:
Mengkuang leaves
Cellulose
Cellulose nanocrystals
Nanoparticles

ABSTRACT

Cellulose was extracted from mengkuang leaves (*pandanus tectorius*) by carrying out alkali and bleaching treatments. Cellulose nanocrystals were isolated from extracted cellulose with concentrated sulphuric acid. The chemical composition of mengkuang leaves was determined at different stages of treatment. Structural analysis was carried out by Fourier transform infrared spectroscopy and X-ray diffraction. Field emission scanning electron microscopy and transmission electron microscopy were used to investigate the morphology of the isolated cellulose and cellulose nanocrystal, respectively. The thermal stability of mengkuang leaves at different stages of treatment was investigated by thermogravimetric analysis. The results indicated that the hemicellulose and lignin were removed extensively from the extracted cellulose. The isolated cellulose and cellulose nanocrystals were found to have diameters in the range 5–80 μm and 5–25 nm, respectively. The thermal stability of the leaves was found to increase at various purification stages when compared to the raw material.

1. Introduction

The use of natural fibres as reinforcements in polymer composites has attracted considerable attention during the last few decades (Abdelmouleh, Boufi, Belgacem, & Dufresne, 2007; Bledzki & Gassan, 1999; Ku, Wang, Pattarachaiyakoop, & Trada, 2011). In addition, natural fibres have applications in fields such as the textile, paper manufacturing, and bioenergy industries owing to their broad availability and properties (Reddy & Yang, 2009; Wambua, Ivens, & Verpoest, 2003).

Natural fibres can generally be classified based on their origin (e.g., plant, animal, or mineral). Plant/vegetable fibres can be further classified into subgroups according to their source (e.g., stem fibres, leaf fibres, seed fibres, or fruit fibres). The chemical composition of plant fibres depends on the type, age, and origin of the fibre, as well as the extraction method. The properties of natural fibres depend on their composition (Bledzki & Gassan, 1999). The major component of plant fibres is cellulose, which is a natural hydrophilic polymer composed of poly(1,4-β-D-anhydroglucopyranose) units. These units contain hydroxyl groups that enable cellulose to establish strong hydrogen bonds. Generally, the most common commercial natural resource that contains cellulose is wood. Several natural fibres such as cotton, flax, hemp, jute, and sisal also contain a large amount of cellulose (Azizi Samir, Alloin, & Dufresne, 2005; Eichhorn et al., 2010). The other major components of natural fibres are hemicelluloses and lignin. Hemicellulose is a branched multiple polysaccharide polymer composed of different types of sugars including glucose, xylose, galactose, arabinose, and mannose. Lignin is a highly crosslinked phenolic polymer. Both hemicellulose and lignin are amorphous polymers, whereas cellulose is a semicrystalline polymer. There are two types of linkages between carbohydrate groups and lignin. One is an ester-type bond between the hydroxyl of lignin and the carboxyl of uronic acid in hemicellulose. This linkage is sensitive to alkali solutions. The second linkage is of the ether type and is formed between the hydroxyls of lignin and those of carbohydrates. Ether-type linkages are insensitive to alkali solutions (Wong & Shanks, 2009).

Removing the amorphous region influences the structure and crystallinity of the fibres. Furthermore, the thermal stability and surface morphology of the fibres are affected by removal of the amorphous parts. Recent studies have shown improvement in the crystallinity and thermal stability during cellulose extraction (Deepa et al., 2011; Li et al., 2009).

Mengkuang is the Malaysian name for *Pandanus tectorius*. It is also known as screw pine, which is a plant belonging to the *Pandanaceae* family. This family has about 600 known species. These species vary in size and grow along mangroves and in local jungles. The fruits can be eaten, and the leaves can be used for weaving. In addition, the leaves yield strong fibres that are used for making rope

* Corresponding author. Tel.: +60 3 8921 5431/5424; fax: +60 3 8921 5410.
E-mail address: gading@ukm.my (I. Ahmad).

0144-8617/$ – see front matter © 2012 Elsevier Ltd. All rights reserved.
doi:10.1016/j.carbpol.2012.01.062

and weaving hats and mats (Giesen, Wulffraat, Zieren, & Scholten, 2006). Although the leaves are widely used in Asia, no studies of the production, composition, or properties of natural cellulose fibres from mengkuang leaves have been conducted to date.

Strong acid hydrolysis is a well-known process for the isolation of nanocrystals from cellulose. Under controlled conditions, acid hydrolysis allows removal of the amorphous regions of cellulose fibres whilst keeping the crystalline domains intact in the form of crystalline nanoparticles. Many different resources have been used to prepare cellulose nanocrystals, such as wood fibres (Beck-Candanedo, Roman, & Gray, 2005), sisal (Garcia de Rodriguez, Thielemans, & Dufresne, 2006; Moran, Alvarez, Cyras, & Vazquez, 2008), pineapple leaves (Cherian et al., 2010), coconut husk fibres (Rosa et al., 2010), and bananas (Deepa et al., 2011). The use of isolated cellulose nanocrystals as reinforcements in the field of nanocomposites has attracted considerable attention since it was first reported by Favier, Chanzy, and Cavaille (1995).

In this study, cellulose and cellulose nanocrystals were extracted from mengkuang leaves by chemical methods. The effects of different chemical treatments on mengkuang leaves were then investigated by Fourier transform infrared (FTIR) spectroscopy, X-ray diffraction (XRD), thermogravimetric analysis (TGA), scanning electron microscopy (SEM), and determination of the chemical composition. The dimensions and aspect ratio of the isolated cellulose nanocrystals were investigated by transmission electron microscopy (TEM).

2. Experimental

2.1. Materials

Mengkuang leaves gathered in Bangi (Selangor, Malaysia) were used in this study. The chemical reagents used were sodium chlorite (purchased from Sigma–Aldrich), acetic acid, sodium hydroxide, sulphuric acid, hydrochloric acid, potassium bromate, sodium thiosulphate, potassium iodide, potassium bromide, ethanol, and benzene (purchased from SYSTERM).

2.2. Extraction of cellulose

The spiny margins and midribs of the leaves were removed, after which the leaves were chopped into approximately 12 cm × 3 cm pieces and partially dried in the sun. The leaves were then placed in stagnant water for three days, during which time the water was changed frequently. The leaves were subsequently boiled for about 15 min, and then washed several times in fresh water. The leaves were finally dried in the sun and ground using a mill. The ground leaves were treated with 4% NaOH at 125 °C for 2 h, after which bleaching treatment was carried out using 1.7 w/v% $NaClO_2$ at pH 4.5 and 125 °C for 4 h. The ratio of the leaves to liquor was 5:100 (g/mL). Each step was repeated several times, and the leaves were washed with distilled water after each treatment.

2.3. Isolation of cellulose nanocrystals

Cellulose nanocrystals were prepared by acid hydrolysis of the cellulose obtained as described elsewhere (Moran et al., 2008). Acid hydrolysis was carried out using 60 wt% H_2SO_4 solution at 45 °C. The time of hydrolysis in this study was fixed at 45 min, which was found to be the optimum time. The ratio of the obtained cellulose to liquor was 5:100 (wt%). The hydrolyzed cellulose sample was washed five times by centrifugation (10,000 rpm, 10 min, and 10 °C) to remove the excess of sulphuric acid. The suspension was then dialyzed against distilled water until a constant pH was reached. The resulting suspension was sonicated for 30 min (Bondeson, Mathew, & Oksman, 2006).

2.4. Characterization

2.4.1. Determination of chemical composition

The chemical composition of mengkuang leaves before and after chemical treatment was investigated. Soxhlet extraction with alcohol–benzene (TAPPI T204) was carried out for 8 h to calculate the content of the extract. The percentage of holocellulose was determined according to the method described by Wise, Murphy, and D'Addieco (1946). The lignin (acid-insoluble) and α-cellulose contents were determined according to TAPPI standard methods T222 and T203, respectively. The pentosan content was determined according to TAPPI standard method T223 as furfural compounds. It should be noted that the procedure used for this standard has been modified by the Forest Research Institute Malaysia (FRIM). Briefly, about 0.6 g of each sample was distilled in 100 mL of 13.2% HCl. The distillation rate was 25 mL/10 min, with an additional 25 mL of HCl added every 10 min until 300 mL of distillate was collected. The distillate was cooled to below 20 °C. A blank was prepared by adding 25 mL of 0.1 N $KBrO_3$ and 10 mL of 10% KBr to 100 mL of the 13.2% HCl. After keeping the solution below 20 °C for 1 h in the dark, 10 mL of 10% KI was added. The sample was then allowed to stand for 5–10 min, after which the solution was titrated with 0.1 N $Na_2S_2O_3$. Each sample was also prepared using the same method, but with distilled HCl instead of 13.2% HCl.

2.4.2. Field emission scanning electron microscopy (FESEM)

A field emission scanning electron microscope (FESEM) (Zeiss Supra 55VP) with an accelerating voltage of 3 kV was used to observe the surface of the longitudinal cross section of dried mengkuang leaves, as well as the leaves after different stages of treatment. All the samples were coated with gold to avoid charging.

2.4.3. Transmission electron microscopy (TEM)

The dimensions of the cellulose nanocrystals were assessed using a Philips CM12 transmission electron microscope operating at 80 kV. Briefly, a drop of a diluted suspension of cellulose nanocrystals was placed on a copper grid coated with a thin carbon film and allowed to dry at room temperature. The nanoparticles were then stained with a 2 wt% solution of uranyl acetate for 1 min and dried at room temperature.

2.4.4. Fourier transform infrared (FTIR) spectroscopy

The FTIR spectra were recorded on a Perkin-Elmer spectrometer (Spectrum GX) in the range 4000–500 cm^{-1} with a scanning resolution of 8 cm^{-1} to investigate possible changes in the functional groups of mengkuang leaves at different stages of extraction. Ground samples were mixed with KBr, after which the mixture was pressed into thin transparent films that were analysed.

2.4.5. X-ray diffraction (XRD)

The crystallinity of mengkuang leaves at different stages of extraction was studied using an X-ray diffractometer (D8 Advance, Bruker AXS) equipped with CuKα radiation (λ = 0.1541 nm) in the 2θ range 10–50°. The operating voltage was 40 kV, and the current was 40 mA. The empirical method (Segal, Creely, Martin, & Conrad, 1959) was used to obtain the crystallinity index of the samples X_c, as shown in Eq. (1):

$$X_c = \frac{I_{002} - I_{am}}{I_{002}} \times 100 \quad (1)$$

where I_{002} and I_{am} are the peak intensities of crystalline and amorphous materials, respectively.

Table 1
Chemical composition of mengkuang leaves at different stages of treatment.

Samples	Cellulose (%)	Hemicellulose (%)	Pentosans (%)	Lignin & ash (%)	Extractive (%)
Mengkuang leaves	37.3 ± 0.6	34.4 ± 0.2	15.7 ± 0.5	24 ± 0.8	2.5 ± 0.02
After alkali treatment	57.5 ± 0.8	15.5 ± 0.1	13.2 ± 0.9	22.6 ± 0.2	–
After bleaching	81.6 ± 0.6	15.9 ± 0.6	12.5 ± 0.6	0.8 ± 0.1	–

2.4.6. Thermogravimetric analysis (TGA)

Thermogravimetric analysis was carried out using a Mettler Toledo model TGA/SDTA851e thermogravimetric analyzer to determine the thermal stability of mengkuang leaves at different stages of extraction. For analysis, the samples were heated from room temperature to 600 °C under a nitrogen atmosphere at 10 °C min^{-1}.

3. Results and discussion

The chemical extraction process affects the chemical composition of the fibres. Starting from raw fibres, the first stage of extraction was alkali treatment. This treatment is supposed to remove and hydrolyze the hemicelluloses, soluble mineral salts, silica, and ash (Deepa et al., 2011; Dufresne, Cavaillé, & Vignon, 1997; Ndazi, Nyahumwa, & Tesha, 2007). The experimental conditions of this alkali treatment influence the morphology of the ensuing material. The results revealed that fibres treated at 130 °C had a smooth surface when compared to fibres obtained at 80 °C (Li et al., 2009) and that 2–4% NaOH was sufficient for this treatment (Ndazi et al., 2007). The second stage was a bleaching treatment. The main goal of bleaching is to remove the lignin (Cherian et al., 2010; Dufresne, Dupeyre, & Vignon, 2000). The bleaching effect depends on the pH and temperature. The reaction occurs at low pH and high temperature.

3.1. Chemical composition

The chemical composition of mengkuang leaves at different stages of treatment is shown in Table 1. The original mengkuang leaves consist of 37.3% α-cellulose, 34.4% hemicellulose, 15.7% pentosans, 24.0% lignin, and 2.5% extractives. After treating the leaves with NaOH solution, the cellulose content increased, whereas the pentosans and lignin were only reduced by about 2%. The alkali treatment affected the content of hemicellulose, which was reduced to 15.5%. This was caused by cleavage of the ester-linked substances of hemicellulose (Deepa et al., 2011; Xiao, Sun, & Sun, 2001). Lignin was extensively removed after five rounds of bleaching, whereas the hemicellulose content was not affected by this treatment. The contents of cellulose, hemicellulose, pentosans, and lignin after bleaching were 81.6%, 15.9%, 12.5%, and 0.8%, respectively.

3.2. Morphological analysis

Fig. 1 shows the mengkuang plant and its leaves at different stages of treatment. The colour of the leaves changed from green to light brown after alkali treatment and became white after bleaching. Fig. 2 shows FESEM micrographs of mengkuang leaves. Microscopic examination of the longitudinal and cross section of the mengkuang leaves is depicted in Fig. 2a–e. Fig. 2c shows a

Fig. 1. Photographs of (a) the mengkuang plant, (b) raw ground leaves, (c) alkali-treated leaves, and (d) bleached leaves.

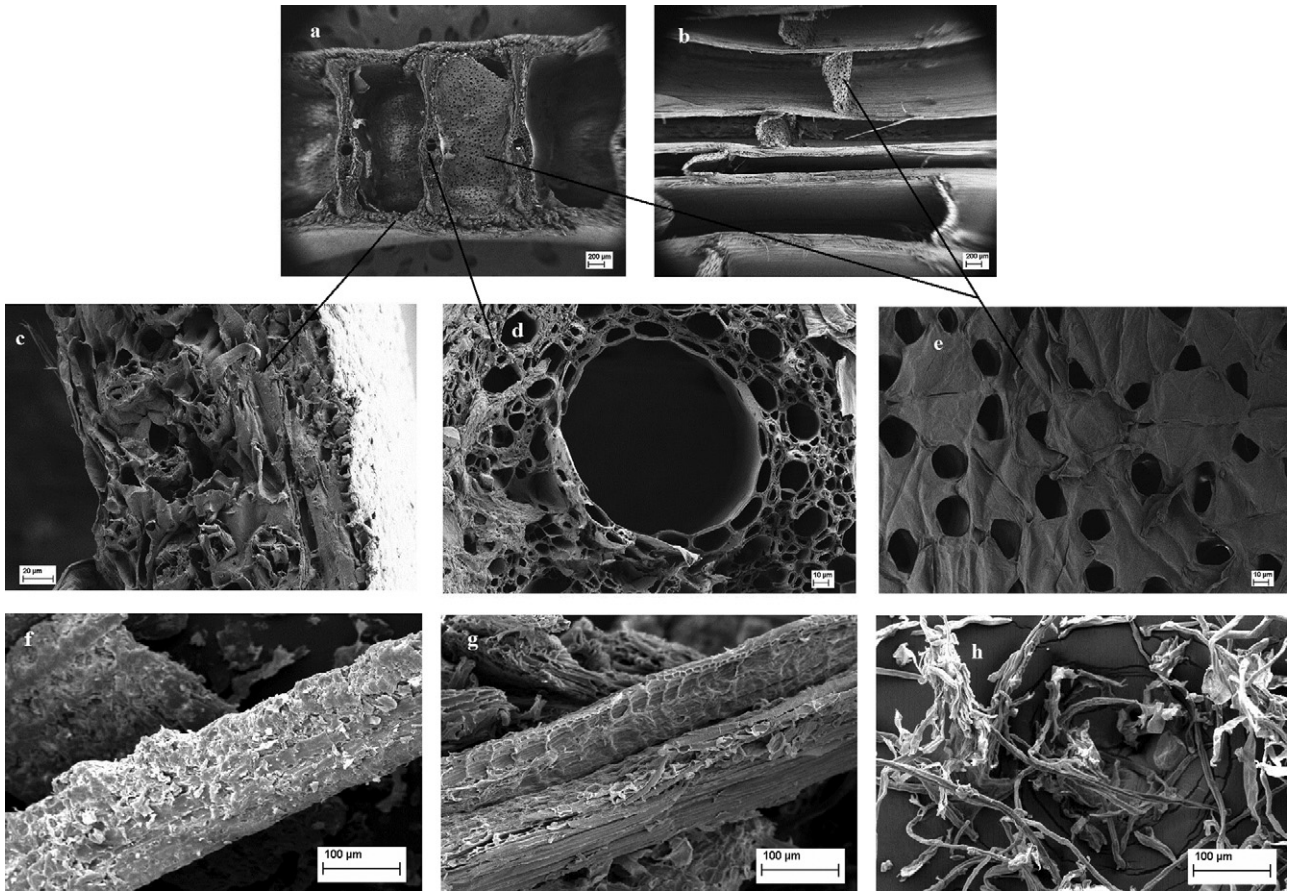

Fig. 2. FESEM micrographs of mengkuang leaves: (a) cross section, (b) longitudinal section, (c) dermal tissue, (d) vascular bundles, (e) ground tissue, (f) raw ground leaves, (g) alkali-treated leaves, and (h) bleached leaves.

dermal tissue with a thickness of around 130 μm, including the cuticle layer and epidermal layer. The interior of the leaf contains vascular bundles (Fig. 2d). Vascular bundles contain xylem and phloem tissues. Xylem is at the centre of the vascular bundles, with the highest diameter being around 150 μm. Xylem conducts water and dissolved minerals. Phloem, which transports photosynthetic products, nutrients, and hormones around the plant, was composed of cells with a diameter in the range 1–22 μm. Xylem and phloem also provide mechanical support to the plant (Strömberg, Guralnick, Simison, Speer, & Cordero, 1998). The interior of the leaf contains also parenchyma (ground tissue) or chlorenchyma tissue called the mesophyll (Fig. 2e). It consists two layers: Palisade layer

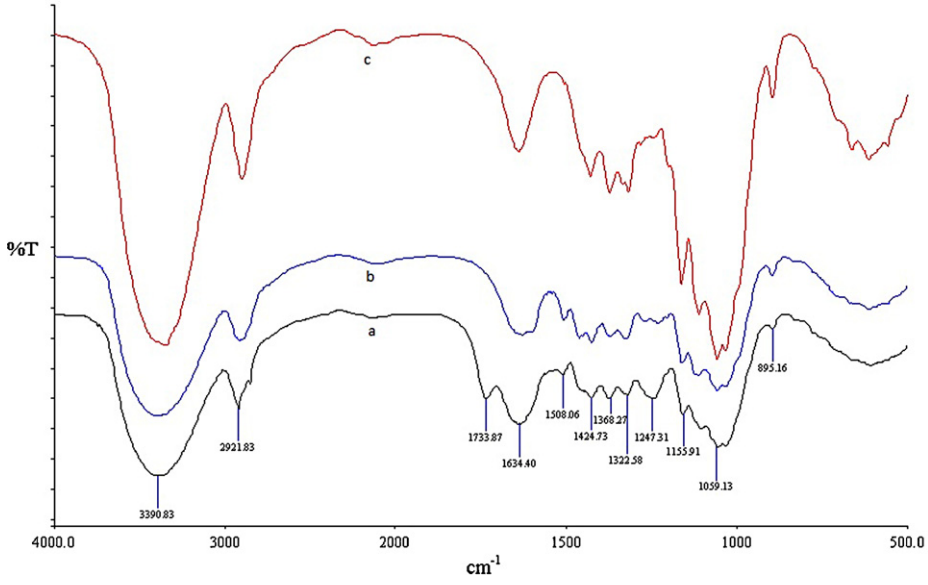

Fig. 3. FTIR spectra of (a) mengkuang leaves, (b) alkali-treated leaves, and (c) bleached leaves.

and spongy layer. These layers could not be distinguished in the micrograph of the dry sample, but it was evident that these tissue cells had lost their protoplasm. The important function of this tissue is photosynthesis (Fahn, 1974).

FESEM micrographs of the raw ground leaves and their products at different stages of extraction (alkali treatment and bleaching) are shown in Fig. 2f–h. The diameters of the fibres in the raw leaves were in the range 100–300 μm. Fig. 2f indicates that fibres in the original leaves were bonded together by cement components, which were partially diminished after the alkali treatment (Fig. 2g). Furthermore, the alkali treatment removed the extractives from the leaves as indicated by the surface changing. After bleaching (Fig. 2h), the fibre bundles where dispersed into individual fibres with diameters in the range 5–80 μm. These images show the partial removal of hemicelluloses and lignin.

3.3. FTIR spectroscopy analysis

Fig. 3 shows the FTIR spectra obtained for mengkuang leaves at different stages of treatment. The band located at 1734 cm^{-1} in the spectrum of raw mengkuang leaves is attributed to C=O stretching of the acetyl and uronic ester groups of hemicellulose or the ester linkage of carboxylic groups of ferulic and p-coumaric acids of lignin and/or hemicellulose (Alemdar & Sain, 2008; Sun, Xu, Sun, Fowler, & Baird, 2005). This band was no longer present in the FTIR spectra of leaves after alkali and subsequent bleaching treatments. The disappearance of this band could have been caused by the removal of hemicellulose and lignin from mengkuang leave fibres during the chemical extraction (Alemdar & Sain, 2008; Jonoobi, Harun, Shakeri, Misra, & Oksman, 2009). However, the results obtained from determination of the chemical composition of the leaves and fibres (Section 3.1 and Table 1) indicate that hemicellulose and lignin were not completely removed after the alkali treatment, and that hemicellulose remained after the bleaching treatment. For this reason, the disappearance of the C=O stretching band from the spectrum could be caused by cleavage of all ester-linked substances of the hemicellulose by alkali treatment. Ether bonds between lignin and hemicellulose were not affected by this treatment (Xiao et al., 2001).

The band at 1508 cm^{-1} that could be seen in the spectrum recorded for raw mengkuang leaves was ascribed to the aromatic C=C stretching from the aromatic ring of lignin. The band observed at 1247 cm^{-1} corresponds to C—O—C (aryl–alkyl ether). These two peaks persisted after the alkali treatment, suggesting that this treatment did not effectively remove lignin. These peaks disappeared after the bleaching treatment, which suggests the removal of lignin (Xiao et al., 2001; Sun et al., 2005). These results were supported by determination of the chemical composition of the fibres.

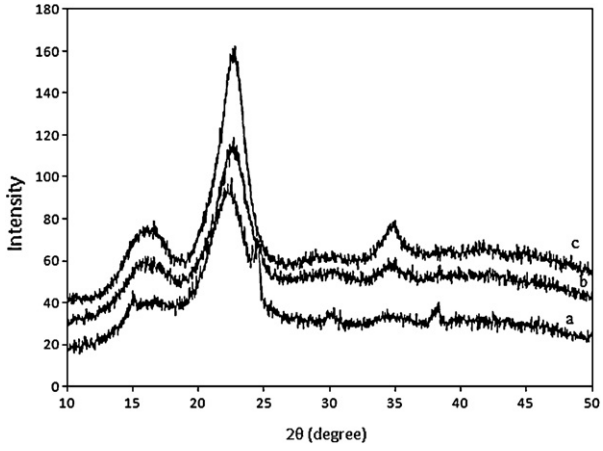

Fig. 4. X-ray diffraction patterns of (a) mengkuang leaves, (b) alkali-treated leaves, and (c) bleached leaves.

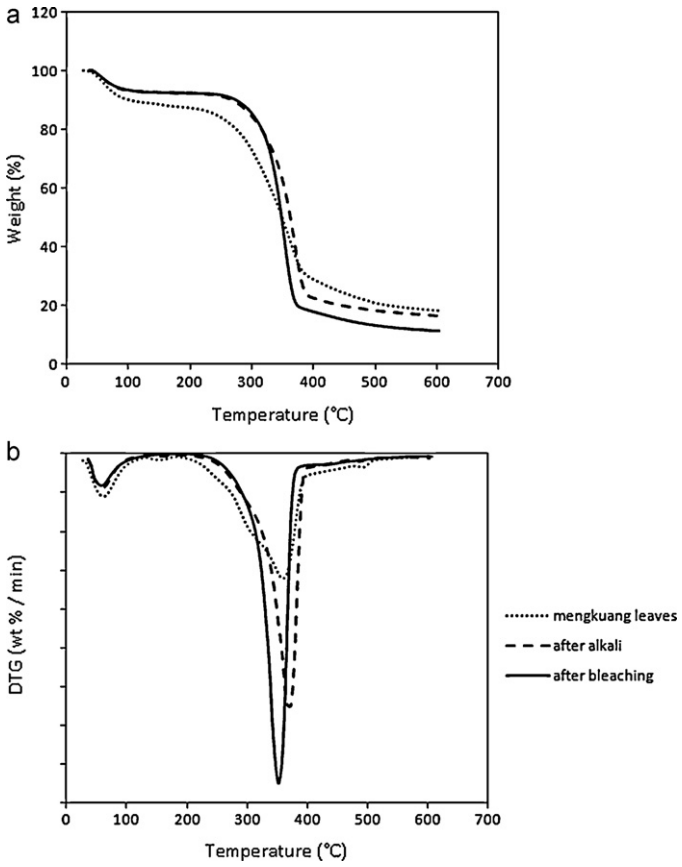

Fig. 5. (a) TG and (b) DTG curves for raw mengkuang leaves, alkali-treated leaves, and bleached leaves.

The absorbance peaks in the region between 1650–1630 cm^{-1} and around 2900 cm^{-1} reflect the stretching of the O—H and C—H groups, respectively. The peaks in the 3400–3300 cm^{-1} region are assigned to the adsorbed water. The two bands around 1060 and 895 cm^{-1} are associated with the C—O stretching and C—H rocking vibrations, respectively, of the carbohydrates (Alemdar & Sain, 2008). These different bands can be seen in all spectra, regardless of the purification of the fibres.

3.4. X-ray diffraction measurements

Both intra- and intermolecular hydrogen bonding occur in cellulose via hydroxyl groups, which results in various ordered crystalline arrangements. Fig. 4 shows the XRD patterns for mengkuang leaves at different stages of treatment. The corresponding crystallinity index values are listed in Table 2. The X-ray diffractograms show that the major intensity peak is located at a 2θ value of around 22.6°, which is related to the crystalline structure of cellulose I for all samples, whilst the amorphous background is characterized by the low diffracted intensity at

Table 2
Crystallinity index of the mengkuang leaves at different stages of treatment.

Samples	2θ (am) (°)	2θ (0 0 2) (°)	X_c%
Mengkuang leaves	18.2	22.5	55.1
After alkali treatment	18.6	22.7	60.2
After bleaching	18.9	22.8	69.5

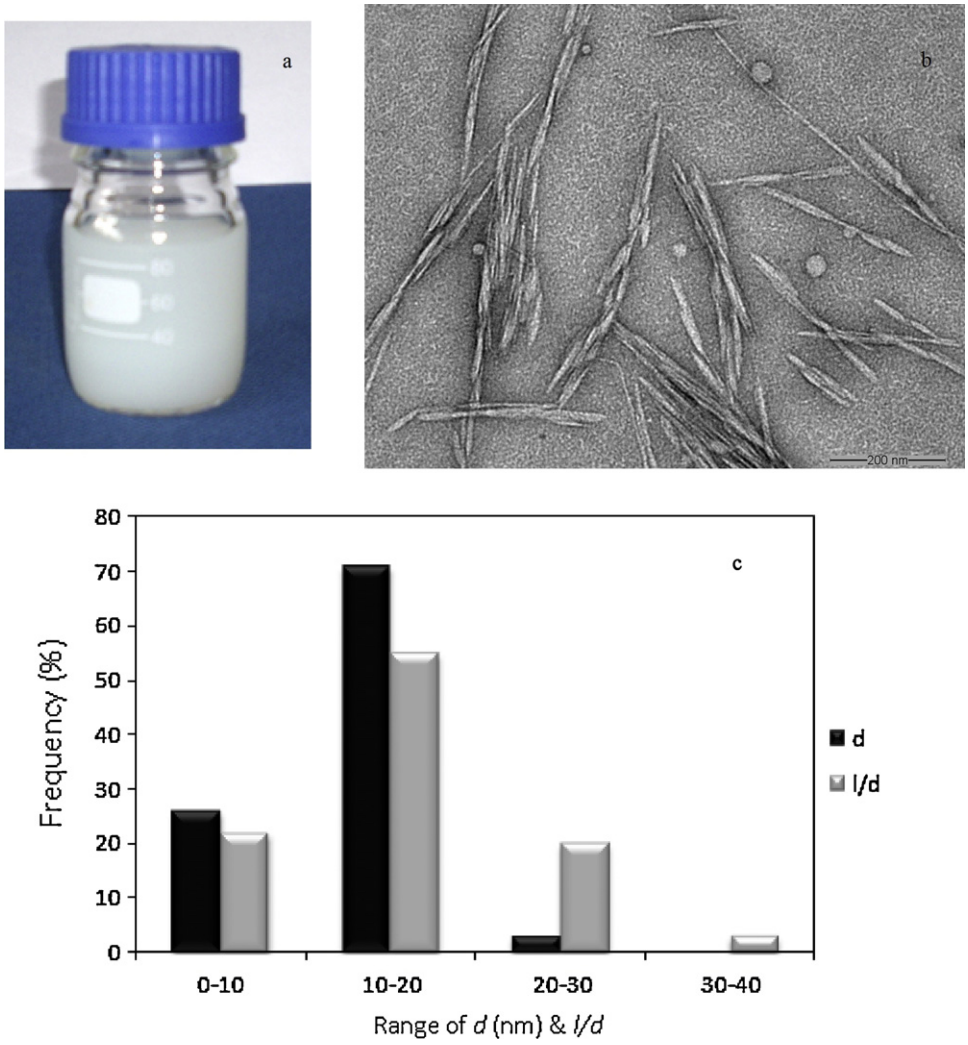

Fig. 6. (a) Aqueous suspension (2 wt%), (b) transmission electron micrograph, and (c) diameter and aspect ratio histograms of cellulose nanocrystals extracted from mengkuang leaves.

a 2θ value of around 18° (Segal et al., 1959). The crystallinity indices of raw leaves, alkali-treated leaves, and bleached leaves were found to be 55.1%, 60.2%, and 69.5%, respectively. These results clearly demonstrate that the crystallinity of the material progressively increases during the chemical extraction. This was ascribed to the progressive removal of amorphous hemicellulose and lignin. The crystallinity index of the sample after bleaching is higher than the value of 54% reported for pineapple leaf fibres by Cherian et al. (2010). However, it is lower than the 75% reported for sisal fibres by Moran et al. (2008). Moreover, the diffraction peak around 22.6° became sharper upon chemical treatment. This observation could reveal better defined crystalline domains.

3.5. Thermogravimetric analysis

Fig. 5 shows the thermogravimetric analysis data obtained for raw mengkuang leaves, as well as those obtained after alkali treatment and bleaching. Both the raw TGA curves (panel a) and derived curves (DTG – panel b) were plotted as a function of temperature. The initial weight loss starting below 100 °C was caused by water evaporation from the samples. The DTG curve for raw mengkuang leaves showed an ill-defined peak around 150 °C. This peak may reflect low molecular weight compounds (Moran et al., 2008). This peak was reduced after alkali treatment and no longer present after bleaching. The curve obtained for raw leaves shows an earlier weight loss starting at around 200 °C. These findings likely reflect the decomposition temperature of hemicelluloses and lignin. Moreover, the weight loss is much more progressive than that of chemically purified samples. In addition, a shoulder is observed in the DTG curve at around 300 °C, but is no longer present after the alkali treatment, which likely reflects the removal of a portion of the hemicellulose.

The degradation temperature after alkali and bleaching treatments is around 250 °C, which is higher than that of raw leaves. However, this value is lower than that reported by Li et al. (2009) for cellulose from mulberry barks and by Soares, Camino, and Levchik (1995) for pure cellulose. This lower degradation temperature could be caused by the hemicellulose component, which remained after the chemical treatments. Hemicellulose is located within and between the cellulose fibrils. This strong association between hemicelluloses and cellulose fibrils is believed to decrease the crystallinity of the cellulose fibrils and accelerate the beginning of the thermal degradation process (Deepa et al., 2011).

The maximum peak temperature in the DTG curves was around 370 °C for both raw mengkuang leaves and alkali-treated samples.

This temperature decreased by about 20 °C upon bleaching. This shift might be because of the residual lignin content (Soares et al., 1995).

3.6. Isolation of cellulose nanocrystals

Acid hydrolysis carried out under appropriate conditions allows the removal of amorphous domains from the cellulosic fibres by cleaving cellulose microfibrils into bundles of cellulose nanocrystals. These nanocrystals, which usually range in length from 100 to 300 nm for many cellulosic materials, become more or less individualized by sonication. The exact dimensions of these nanocrystals depend on the source of cellulose and hydrolysis conditions (Eichhorn et al., 2010). The yield of cellulose nanocrystal was about 28% after 45 min of hydrolysis. It is well known that the use of sulphuric acid for hydrolysis treatment provides isolated crystalline fragments and imparts a charged surface. These charges induce electrostatic repulsion forces between nanoparticles, which lead to a stable aqueous suspension (Azizi Samir, Alloin, Sanchez, & Dufresne, 2004; Bondeson et al., 2006).

The ensuing suspension of isolated cellulose nanocrystal prepared from purified mengkuang fibres is shown in Fig. 6a. The concentration of this suspension was 2 wt%. TEM observation and the distribution of diameters and aspect ratios are shown in Fig. 6b and c, respectively. Mengkuang cellulose nanocrystals ranged in length from 50 to 400 nm, with an average value around 200 nm. The diameter was in the range 5–25 nm. This diameter was lower than that reported for cellulose nanocrystals extracted from sisal fibres (30.9 ± 12.5 nm) by Moran et al. (2008). These results demonstrate the efficiency of the conditions used for the acid hydrolysis treatment of mengkuang fibres and confirm that the aqueous suspension contained individual nanocrystals. The highest fraction (around 55%) of cellulose nanocrystals has an aspect ratio in the range 10–20. This value is quite low when compared to the value of 60 reported for sisal cellulose whiskers by Garcia de Rodriguez et al. (2006). However, the value observed here is similar to the aspect ratio values reported for cellulose nanocrystals extracted from alfa (Ben Elmabrouk, Thielemans, Dufresne, & Boufi, 2009), cotton (Ebeling et al., 1999), Curaúa (Corrêa, Teixeira, Pessan, & Mattoso, 2010), and flax (Cao, Dong, & Li, 2007). The result also showed that based on cellulose content, the leaves consist about 10.4% of cellulose nanocrystals.

4. Conclusion

Extraction of cellulose and isolation of cellulose nanocrystals from mengkuang leaves were successfully carried out by chemical methods. Determination of the chemical composition and microscopic observation showed the effects of chemical treatments on the surface and components of mengkuang leaves. Upon treatment, both the cellulose content and crystallinity of the fibres increased. The crystallinity of the extracted cellulose was 69.5%. The thermal stability of mengkuang leaf fibres increased after chemical treatments. TEM observation revealed that mengkuang leaves can be used as a starting material for the preparation of cellulose nanocrystals. They were found to have an average length of around 200 nm and an aspect ratio in the range 10–20.

Acknowledgments

This study was supported by research grants from the Ministry of Science, Technology and Innovation (MOSTI), Ministry of Higher Education (MOHE), and Universiti Kebangsaan Malaysia. The authors are grateful to Mr. Hasanudin Saleh for sampling the leaves. The authors also thank the Forest Research Institute Malaysia (FRIM) and Mrs. Thureia A. El-Sharif for their advice and fruitful discussions. Additionally, Rasha M. El. Sheltami thanks the Ministry of Higher Education of Libya for providing a scholarship. The French Embassy in Kuala Lumpur is also acknowledged for financial support (French Scholars in Malaysia).

References

Abdelmouleh, M., Boufi, S., Belgacem, M. N., & Dufresne, A. (2007). Short natural-fibre reinforced polyethylene and natural rubber composites: Effect of silane coupling agents and fibres loading. *Composites Science and Technology*, *67*, 1627–1639.

Alemdar, A., & Sain, M. (2008). Isolation and characterization of nanofibers from agricultural residues – wheat straw and soy hulls. *Bioresource Technology*, *99*, 1664–1671.

Azizi Samir, M. A. S., Alloin, F., & Dufresne, A. (2005). Review of recent research into cellulosic whiskers, their properties and their application in nanocomposite field. *Biomacromolecules*, *6*, 612–626.

Azizi Samir, M. A. S., Alloin, F., Sanchez, J.-Y., & Dufresne, A. (2004). Cellulose nanocrystals reinforced poly(oxyethylene). *Polymer*, *45*, 4149–4157.

Beck-Candanedo, S., Roman, M., & Gray, D. G. (2005). Effect of reaction conditions on the properties and behavior of wood cellulose nanocrystal suspensions. *Biomacromolecules*, *6*, 1048–1054.

Ben Elmabrouk, A., Thielemans, W., Dufresne, A., & Boufi, S. (2009). Preparation of poly(styrene-co-hexylacrylate)/cellulose whiskers nanocomposites via miniemulsion polymerization. *Journal of Applied Polymer Science*, *114*, 2946–2955.

Bledzki, A. K., & Gassan, J. (1999). Composites reinforced with cellulose based fibres. *Progress in Polymer Science*, *24*, 221–274.

Bondeson, D., Mathew, A., & Oksman, K. (2006). Optimization of the isolation of nanocrystals from microcrystalline cellulose by acid hydrolysis. *Cellulose*, *13*, 171–180.

Cao, X., Dong, H., & Li, C. M. (2007). New nanocomposite materials reinforced with flax cellulose nanocrystals in waterborne polyurethane. *Biomacromolecules*, *8*, 899–904.

Cherian, B. M., Leão, A. L., de Souza, S. F., Thomas, S., Pothan, L. A., & Kottaisamy, M. (2010). Isolation of nanocellulose from pineapple leaf fibres by steam explosion. *Carbohydrate Polymers*, *81*, 720–725.

Corrêa, A. C., Teixeira, E. M., Pessan, L. A., & Mattoso, L. H. C. (2010). Cellulose nanofibers from curaua fibers. *Cellulose*, *17*, 1183–1192.

Deepa, B., Abraham, E., Cherian, B. M., Bismarck, A., Blaker, J. J., Pothan, L. A., et al. (2011). Structure, morphology and thermal characteristics of banana nano fibers obtained by steam explosion. *Bioresource Technology*, *102*, 1988–1997.

Dufresne, A., Cavaillé, J. Y., & Vignon, M. R. (1997). Mechanical behavior of sheets prepared from sugar beet cellulose microfibrils. *Journal of Applied Polymer Science*, *64*, 1185–1194.

Dufresne, A., Dupeyre, D., & Vignon, M. R. (2000). Cellulose microfibrils from potato tuber cells: Processing and characterization of starch–cellulose microfibril composites. *Journal of Applied Polymer Science*, *76*, 2080–2092.

Ebeling, T., Paillet, M., Borsali, R., Diat, O., Dufresne, A., Cavaillé, J. Y., et al. (1999). Shear-induced orientation phenomena in suspensions of cellulose microcrystals, revealed by small angle X-ray scattering. *Langmuir*, *15*, 6123–6126.

Eichhorn, S. J., Dufresne, A., Aranguren, M., Marcovich, N. E., Capadona, J. R., Rowan, S. J., et al. (2010). Review: Current international research into cellulose nanofibres and nanocomposites. *Journal of Materials Science*, *45*, 1–33.

Fahn, A. (1974). *Plant anatomy* (2nd ed.). Pergamon Press., pp. 235–278.

Favier, V., Chanzy, H., & Cavaille, J. Y. (1995). Polymer nanocomposites reinforced by cellulose whiskers. *Macromolecules*, *28*, 6365–6367.

Garcia de Rodriguez, N. L., Thielemans, W., & Dufresne, A. (2006). Sisal cellulose whiskers reinforced polyvinyl acetate nanocomposites. *Cellulose*, *13*(3), 261–270.

Giesen, W., Wulffraat, S., Zieren, M., & Scholten, L. (2006). *Mangrove guidebook for Southeast Asia, (part II)*. The Netherlands: FAO and Wetlands International., 2006/07.

Jonoobi, M., Harun, J., Shakeri, A., Misra, M., & Oksman, K. (2009). Chemical composition, crystallinity, and thermal degradation of bleached and unbleached kenaf bast (*Hibiscus cannabinus*) pulp and nanofibers. *BioResources*, *4*(2), 626–639.

Ku, H., Wang, H., Pattarachaiyakoop, N., & Trada, M. (2011). A review on the tensile properties of natural fiber reinforced polymer composites. *Composites Part B: Engineering*, *42*(4), 856–873.

Li, R., Fei, J., Cai, Y., Li, Y., Feng, J., & Yao, J. (2009). Cellulose whiskers extracted from mulberry: A novel biomass production. *Carbohydrate Polymers*, *76*(1), 94–99.

Moran, J. I., Alvarez, V. A., Cyras, V. P., & Vazquez, A. (2008). Extraction of cellulose and preparation of nanocellulose from sisal fibers. *Cellulose*, *15*(1), 149–159.

Ndazi, B. S., Nyahumwa, C., & Tesha, J. (2007). Chemical and thermal stability of rice husks against alkali treatment. *BioResources*, *3*(4), 1267–1277.

Reddy, N., & Yang, Y. (2009). Properties of natural cellulose fibers from hop stems. *Carbohydrate Polymers*, *77*(4), 898–902.

Rosa, M. F., Medeiros, E. S., Malmonge, J. A., Gregorski, K. S., Wood, D. F., Mattoso, L. H. C., et al. (2010). Cellulose nanowhiskers from coconut husk fibers: Effect of preparation conditions on their thermal and morphological behavior. *Carbohydrate Polymers*, *81*(1), 83–92.

Segal, L., Creely, J. J., Martin, A. E., & Conrad, C. M. (1959). An empirical method for estimating the degree of crystallinity of native cellulose using the X-ray diffractometer. *Textile Research Journal*, *29*(10), 786–794.

Soares, S., Camino, G., & Levchik, S. (1995). Comparative study of the thermal decomposition of pure cellulose and pulp paper. *Polymer Degradation and Stability*, *49*(2), 275–283.

Strömberg, C., Guralnick, R., Simison, B., Speer, B., & Cordero, A. (1998). *Laboratory I: Introduction to plant structure*. Berkeley: The Museum of Paleontology of the University of California. http://www.ucmp.berkeley.edu/IB181/VPL/Ana/AnaTitle.html

Sun, X. F., Xu, F., Sun, R. C., Fowler, P., & Baird, M. S. (2005). Characteristics of degraded cellulose obtained from steam-exploded wheat straw. *Carbohydrate Research*, *340*(1), 97–106.

Wambua, P., Ivens, J., & Verpoest, I. (2003). Natural fibres: Can they replace glass in fibre reinforced plastics? *Composites Science and Technology*, *63*(9), 1259–1264.

Wise, L. E., Murphy, M., & D'Addieco, A. A. (1946). Chlorite, holocellulose, its fractionation and bearing on summative wood analysis and on studies on the hemicellulose. *Paper Trade Journal*, *122*(2), 35–43.

Wong, S., & Shanks, R. (2009). Biocomposites of natural fibers and poly(3-hydroxybutyrate) and copolymers: Improved mechanical properties through compatibilization at the interface. In L. Yu (Ed.), *Biodegradable polymer blends and composites from renewable resources* (pp. 303–347). New Jersey: John Wiley & Sons, Inc.

Xiao, B., Sun, X. F., & Sun, R. (2001). Chemical, structural, and thermal characterizations of alkali-soluble lignins and hemicelluloses, and cellulose from maize stems, rye straw, and rice straw. *Polymer Degradation and Stability*, *74*(2), 307–319.